Biogeosciences

Dissolution of cobalt and zinc from natural and anthropogenic dusts in seawater

C.-E. Thuróczy[1,*], M. Boye[1], and R. Losno[2]

[1]Laboratoire des sciences de l'Environnement MARin CNRS UMR6539, Institut Universitaire Européen de la Mer, Place Nicolas Copernic, Technopôle Brest-Iroise 29280 Plouzané, France
[2]LISA Université Paris-Diderot et Paris Est Créteil, UMR CNRS 7583, 61 avenue du Général de Gaulle, 94010 Créteil Cedex, France
*present address: Royal Netherlands Institute for Sea Research, P.O. Box 59, 1790 AB Den Burg (Texel), The Netherlands

Abstract. Atmospheric dust inputs to the surface ocean are a major source of trace metals likely to be bio-available for phytoplankton after their dissolution in seawater. Among them, cobalt (Co) and zinc (Zn) are essential for phytoplankton growth and for the distribution of the major groups such as coccolithophorids, cyanobacteria and diatoms. The solubility in seawater of Co and Zn present in natural and anthropogenic dusts was studied using an open-flow reactor with and without light irradiation. Those dusts can be transported in the atmosphere by the wind before being deposited to the surface ocean. The analyses of cobalt and zinc were conducted using voltammetric methods and the global elemental composition of dust was determined by ICP-AES. This study highlighted the role of the dust origin in revealing the solubility characteristics. Much higher dust solubility was found for zinc as compared to cobalt; cobalt in anthropogenic particles was much more soluble (0.78%) in seawater after 2 h of dissolution than Co in natural particles (0.14%). Zinc showed opposite solubility, higher in natural particles (16%) than in anthropogenic particles (5.2%). A natural dust event to the surface ocean could account for up to 5% of the cobalt inventory and up to 50% of the Zn inventory in the mixed layer in the Pacific Ocean whereas the cobalt and zinc inventories in the mixed layer of the Atlantic Ocean might already include the effects of natural dust inputs and the subsequent metal dissolution. Anthropogenic sources to the surface ocean could be as important as the natural sources, but

a better estimate of the flux of anthropogenic aerosol to the surface ocean is needed to further estimate the anthropogenic inputs. Variations in natural and anthropogenic inputs may induce large shifts in the Co/Zn ratio in the surface ocean; hence it could impact the phytoplankton community structure.

1 Introduction

Atmospheric inputs of dust to the open surface ocean are a major source of metals and nutrients (Duce and Tindale, 1991; Jickells et al., 2005). River inputs and upwelling can also be an important source of trace metals (Johnson et al., 1997). Atmospheric sources of dust is generated by the erosion of land surfaces (wind transported dusts), but also by direct emission from anthropogenic activities (industry, agriculture, transportation). The dissolution of these natural and anthropogenic particles in the upper layer of the ocean can vary with their origin, their elemental composition and the possible transformation which can occur in acid clouds of the atmosphere and/or by UV irradiation. Bio-available trace metals can regulate the growth of the phytoplankton influencing the primary production and the carbon cycle (Sunda and Huntsman, 1995). The nutritive metals contained in dust can be available for phytoplankton after their dissolution in seawater. Among these micro-nutrients, cobalt (Co) and zinc (Zn) have a potential key role in phytoplankton physiology and productivity. For instance the distribution of dissolved Zn in seawater shows nutrient-like profile (such as phosphate and silicate; Saito and Moffett, 2002) whereas

Co shows a hybrid-type profile, combining nutrient-like and scavenged-like vertical distribution (Noble et al., 2008). Furthermore the growth rate of coccolithophorids, like *Emiliania huxleyi*, and cyanobacteria, like *Prochlorococcus* and *Synechococcus*, can be primarily limited by the low Co concentrations (Sunda and Huntsman, 1995; Saito et al., 2002). In contrast Zn would be primarily requested for the growth of diatoms, rather than Co (Sunda and Huntsman, 1995). Both Zn and Co play important roles in the physiology of the phytoplankton (Frausto da Silva and Williams, 1994) like in the DNA replication (Zn-fingers), in enzyme activity (carbonic anhydrase; Vallee and Auld, 1990) and in the structure of vitamins (for instance Co is the co-factor in the B_{12} vitamin; Kobayashi and Shimizu, 1999). Thus, Co and Zn inputs to the surface ocean can impact the growth, some metabolic processes, the phytoplankton community structure and the carbon flux at the atmosphere-ocean interface. However the solubility and the biogeochemical impact of these trace metals is still poorly described or virtually unknown.

The dissolution of trace metals could depend on the origin of the particles, on their size, on the type of deposition (dry or wet) and on the pH of the rains (Desboeufs and Losno, 2001; Bonnet and Guieu, 2004; Journet et al., 2008). For instance metals contained in carbonated dusts are more easily dissolved in water than those present in alumino-silicate particles due to different binding strength of the metal to the mould (Desboeufs et al., 2005). So far studies on the dissolution of trace metals have been mainly focusing on iron and have been performed in enclosed systems (Bonnet and Guieu, 2004). Such enclosed experiments have shown that there is a possible saturation of dissolved metal in the water (Bonnet and Guieu, 2004) that does not mimic the processes taking place in the surface ocean. Furthermore most of the experiments were done in pure water, and next with different pH to simulate the rains (Desboeufs, 2001a; Desboeufs et al., 1999, 2001), which does not fit with the chemical dynamics of the surface ocean. This work aims to determine the solubility of Co and Zn contained in atmospheric dusts (dust transported by the wind) from different origins in seawater using an open-flow reactor, and the effect of photochemical processes on the dissolution of these trace metals.

2 Material and methods

2.1 Particles sampling

Two types of particles for aerosol simulation were considered here. All dust samples (anthropogenic and natural) were sieved using different size fractions between >500 μm and <20 μm. The smallest fraction (<20 μm) was studied as it is the most representative fraction available here of the wind-transported material and due to the size sieves available and the sieving method which must be dry sieving. The fine fraction (<20 μm, sieved from bulk) of a crustal soil originated
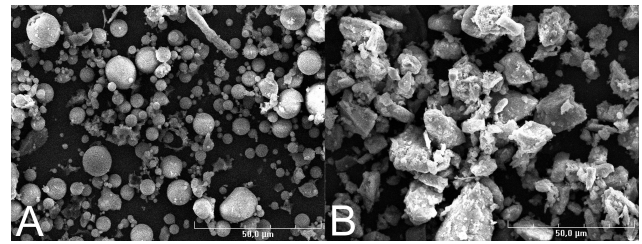

Fig. 1. SEM (Scanning Electron Microscopy) pictures of anthropogenic coal ash dust (**A**) and of natural loess from Cape Verde (**B**). Pictures obtained with the collaboration of the Electronic Microscopy Group, Université de Bretagne Occidentale, Brest, France.

from Cape Verde Islands (a loess similar to Saharan soil) was used for simulation of natural mineral aerosol. These collected soil samples were exposed to scarce rains at Sal Island. Crustal dusts from other locations (such as in Desboeufs et al., 1999) are also influenced by rain and erosion before being transported by the wind in the atmosphere, thus they are comparable to our samples. The anthropogenic material, a coal ash dust, was flying ashes collected in electrostatic separators before exhaust in a power plant (Le Havre, France), where combustion was almost completed. It was used for simulation of an anthropogenic aerosol. The differences in morphology between these natural and anthropogenic particles are shown in Fig. 1. It showed small-size particles with a regular and spherical structure for the coal ash dust and a heterogeneous structure for the natural soil.

2.2 Experimental device

The dissolution experiments of trace metals in seawater was performed using an open-flow reactor to avoid saturation effects, in order to better mimic the natural processes occurring in the surface ocean with or without light irradiation. It was constituted of a constant volume pump (giving a flow rate, F, between approximately 14 mL/min at the start of the experiment and 8 mL/min at the end depending on the amount of particles present in the chamber), a reaction chamber (V=73.7 mL) ended by a membrane filter (Whatman polycarbonate 0.4 μm, acid cleaned, 47 mm diameter) and an exhaust tubing (Desboeufs et al., 1999; Desboeufs, 2001a; Velay, 2006). This reactor allowed a permanent non-stationary system by using a continuous flow of seawater on the particles thus preventing from saturation of the dissolved phase. This system is inspired from a paper published by Chou and Wollast (1984). The reactor and all the tubings were PTFE material and acid cleaned. The irradiation device consisted of a 125 W high-pressure xenon bow-lamp recreating the solar spectrum (Model 125 W MSR) but with some blue-UV enrichment. The light was brought to the reactor through an optical fiber. The actinic flux in the blue-close UV measured from H_2O_2 decomposition was 10 to 20 times higher than the natural irradiation found with a bright weather (Velay, 2006).

The seawater used for all the experiments was collected in a HNLC area in the mixed layer at the chlorophyll maximum depth during the KEOPS cruise aboard R.V. Marion-Dufresne in 2005 with ultra-clean conditions and using a kevlar wire and GO-FLO bottles (Blain et al., 2007). Twenty liters were filtered on board using 0.2 µm cut-off filter (Sartorius Sartobran cartridge) and stored in one ultra-clean Nalgene bottles (LDPE) in the dark. The 20 L HNLC bulk water was stirred before use. Because of the pore size of the filter (0.2 µm) it is unlikely that microorganisms were present in the seawater used for the dissolution experiments and therefore would have any effect on the results. On the other hand if there was any effect of dissolved organic matter it was the same for every experiment.

For both particle types, Zn and Co dissolution experiments were conducted under light irradiation, and also in the dark for the Co dissolution.

Around 20 mg of solid phase was weighted and put at the bottom of the reactor under a magnetic stick stirrer. The experiment started when the seawater reached the reactor and was followed during 2 h with a continuous seawater flow. Dissolved samples (<0.4 µm) were collected in acid cleaned LDPE Nalgene bottles (60 mL) at the outlet of the reactor. Sampling frequency was every 2 min during the first 20 min of the experiment, after which samples were taken at 30, 45, 60, 90 and 120 min. They were immediately acidified to pH 2 with Suprapur[TM] HCl (Merck) and stored at room temperature in the dark before being analyzed by voltammetry. All the experiments were done in an ISO3 clean room, under an ISO1 laminar flow hood.

2.3 Determination of the dust elemental composition

The elemental composition of the dust samples was determined by ICP-AES (Type Optima 3000, Perkin-Elmer) after their mineralization. The mineralization of 60 to 80 mg of particles was performed in ultra-clean Teflon bottles using 2 mL hydrochloric acid 30%, 2 mL of hydrofluoro acid 40% and 2 mL of 65% nitric acid (Normapur™ from Prolabo). The digestion was performed at 50 °C for one day under a fume hood. The acids were left for evaporation at 150 °C. Then, 2 mL of 65% nitric acid were added at 50 °C and the bottles closed for a day. This last sample was diluted in 60 mL of milli-Q[TM] water in a clean room. The samples were diluted 10 to 15 times to adjust the concentration to the ICP-AES requirements. Blank samples were prepared without particles using the same protocol used for the dust mineralization to test the cleanliness of the protocol (Annexe 1).

2.4 Determination of the dissolution rates of trace metals in seawater

Dissolved Zn and Co concentrations were determined in filtered seawater (Whatman polycarbonate 0.4 µm, mounted downstream of the open-flow reactor) by Anodic and Ca-thodic Stripping Voltammetry, respectively (ASV and CSV). The voltammetric equipment consisted of a µAutolab potentiostat (Type III, Ecochemie) connected to a hanging mercury drop electrode (model VA 663 from Metrohm). The mercury drop size was approximately $0.52\,mm^2$. The reference electrode was double-junction, Ag/AgCl, 3 M KCl, with a salt bridge filled with 3 M KCl and a glassy carbon counter-electrode. Samples were stirred with a PTFE Teflon stirrer (2500 rpm). Each equilibrated sample was poured into the voltammetric measurement cell and analyzed following the procedures indicated in Table 1. The samples were brought back to pH 8.2 before analyzing using a 1.5 M borate buffer prepared in 0.4 M NaOH solution. Zn was complexed by APDC (Ammonium Pyrrolidine Dithio Carbamate; Ellwood and van den Berg, 2000). A 0.0013 M stock was prepared in Q-NH$_3$ 0.1%. The final concentration in the sample was 60 µM. Co was complexed by nioxime (1,2-cyclohexanedione dioxime; Ellwood and van den Berg, 2001). A first 0.1 M stock was prepared in 0.2 M NaOH and a second one (40 µM) was prepared by diluting the first one. The final concentration in the sample was 800 nM.

The voltammetric analyses were calibrated against the NASS-4 certified seawater (calibrated with both "Inductively Coupled Plasma-Mass Spectrometry" and "Graphite Furnace Atomic Absorption Spectrometry"). The concentrations of Co and Zn determined by voltammetry were of the same order (Co: 0.26 ± 0.02 nM, $n=3$; Zn: 1.69 ± 0.29 nM, $n=3$) as the certified values (Co: 0.15 ± 0.02 nM; Zn: 1.75 ± 0.27 nM). However, the Co concentration found by voltammetry was slightly higher.

The background concentrations (e.g., $[X]_{in}$, see below Eq. 1) in the HNLC filtered (<0.2 µm) bulk seawater used for the dissolution experiments measured by voltammetry were 0.049 ± 0.007 nM ($n=4$) for Co and 0.845 ± 0.047 nM ($n=3$) for Zn. Hence the detection limits estimated as three time the standard deviations of replicate analyses in such filtered HNLC seawater were 0.022 nM for Co, close to those reported by Westerbrink et al. (1990), and 0.142 nM for Zn.

Blanks were performed by running the dissolution reactor without any dust inside. Blanks were also performed with the sub-sampling bottles. No contamination was detected, either for Co or for Zn. All these experiments and analyses were done in clean rooms with ultra-clean procedures and material (including acid washed sampling bottles, clean sampling seawater, acid clean filters, etc...).

3 Results

3.1 Elemental composition of the particles

The elemental composition determined by ICP-AES (Table 2, Annexe 2) of the dusts did not vary significantly between natural and anthropogenic dust for Co, but anthropogenic dust was enriched in Zn. Consequently the

Table 1. Voltammetric procedures for Zn and Co determinations.

	Method	Zn Square wave	Co Differential pulse
Pre-treatment	Purge time (s)	300	300
	Conditionning potential (V)	−1.2	−0.7
	Duration (s)	120	180
	Deposition potential (V)	−1	−1
	Duration (s)	1	1
	Equilibration time (s)	10	10
Measurement	Frequency Hz	50	/
	Modulation time	/	0.01
	Interval time	/	0.1
Potentials (V)	Initial	−1.15	−0.7
	End	−0.75	−1.3
	Step	0.003	0.0048–0.0096
	Amplitude	0.01995	0.04995
	Standby	0	0

Table 2. Elemental composition in Co and Zn of the natural and anthropogenic dust samples as determined by ICP-AES (µg/g and µmol/g) and ratio [Co]/[Zn].

	Loess	Coal ash dust
[Co] (µg/g)	181.76	212.77
[Co] (µmol/g)	3.09	3.61
[Zn] (µg/g)	102.39	744.19
[Zn] (µmol/g)	1.57	11.38
[Co]/[Zn] (weight)	1.78	0.29
[Co]/[Zn] (molar)	1.97	0.32

elemental ratio [Co]/[Zn] (Table 2) was much higher in the natural dusts (1.78 in weight) compared to the coal ash dusts (0.29 in weight).

3.2 Dissolution from dust in seawater

Co and Zn concentrations ([X]) were measured by voltammetry for each of the kinetic experiment sample. From these measured concentrations, the dissolution rate of the element X can be computed by the following equation:

$$DR_X = F([X]_{out}-[X]_{in}) + V d[X]_{out}/dt \qquad (1)$$

Where DR_X is the dissolution rate of the element X (mol/min), F the flow rate (L/min), $[X]_{in}$ and $[X]_{out}$ the respective dissolved concentrations (mol/L) in seawater at the input (e.g., background concentration, see values here above) and the output of the dissolution reactor (Annexes 3 and 4), V the volume of the dissolution cell (L) and t the time (min). The Eq. (1) describes an open flow reactor. The first term, F ($[X]_{out} - [X]_{in}$), is the dilution of the soluble element in the reaction cell from the dust; and the second term, $V d[X]_{out}/dt$, is the dilution effect of the solution in the reaction cell by the new solution input. In case of a steady state, $[X]_{out}$ is constant and the second term is null, but it was never the case in our experiments.

For discrete sampling, the second term in the Eq. (1) can be approximated by:

$$V d[X]_{out}/dt = V([X]_{out(i+1)}-[X]_{out(i)})/(t_{i+1}-t_i) \qquad (2)$$

except for the first sample where DR is calculated by: $DR = V([X]_{out}-[X]_{in})/t_0$, where t_0 is the duration of the dissolution cell filling.

The dissolution rate can be expressed as a relative dissolution rate (RDR_X %) with:

$$RDR_X\% = DR_X/m_X \qquad (3)$$

Where m_X (mol) is the amount of element X introduced as part of the dust in the dissolution chamber. Figures 2 and 5 show the dissolution rate as function of time for Co and Zn in the anthropogenic and natural dust.

Cumulated dissolution (CD_i, results reported in Figs. 3 and 6) is calculated step by step as shown in the following equation (Eq. 4) at time $(t_i+t_{i-1})/2$:

$$CD_i = CD_{i-1} + DR(t_i) \cdot (t_i - t_{i-1}) \qquad (4)$$

The first step CD_0 is calculated separately as: $CD_0 = V([X]_{out}-[X]_{in})$.

The uncertainties reported on the graphs (Figs. 2 to 7) were calculated from the uncertainties measured in the concentrations using uncertainties propagation formulas in Eqs. (1), (2) and (4) for the dissolution rate graphs. One experiment was done for each condition due to the restricted volume of HNLC seawater available, but replicates were made for the metals analyses. Analytical uncertainties are calculated by computing analytical replicates done for each sample.

3.3 Cobalt in seawater

The dissolution rate of anthropogenic Co (Fig. 2) varied from 0.06%/min at the beginning of the dissolution experiment to values below 0.01%/min after 20 min of experiment. No clear differences were observed between illuminated and dark experiments. A quite different behaviour was observed for natural Co. Despite a similar elemental proportion of Co in coal ash and natural dust, the Co dissolution rate at the beginning was ten times lower in loess (0.007%/min) than in coal ash dust. But the dissolution rate decreased a bit during the first 30 min, and then increased again after one hour to reach 0.003%/min at the end. The irradiation seemed to produce a noticeable effect at the beginning of the experience only with slightly higher dissolution rate. However the Co concentrations obtained with the loess were in the same range than the concentration already detected in seawater, introducing bias in the precision of the calculated dissolution rate as shown with the large uncertainty intervals plotted on Fig. 2.

The dissolution rate measured with the open flow reactor can be integrated over the experience time giving cumulative solubility (Fig. 3). This solubility was much higher for the
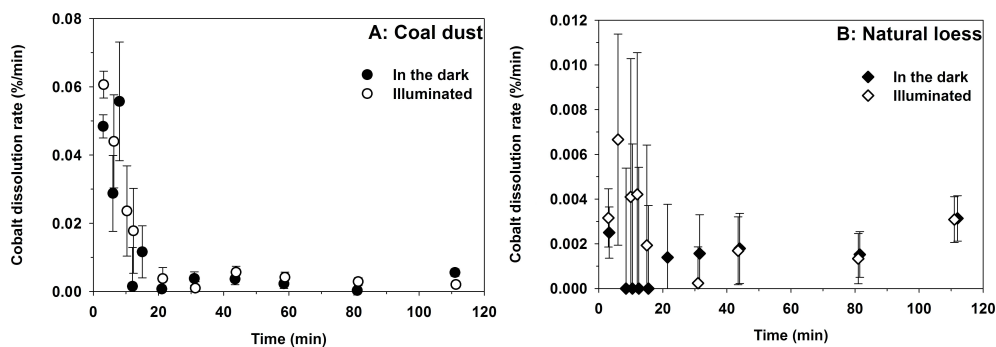
Fig. 2. Dissolution rates of cobalt (%/min) for anthropogenic (**A**) and natural (**B**) dust expressed as function of time.
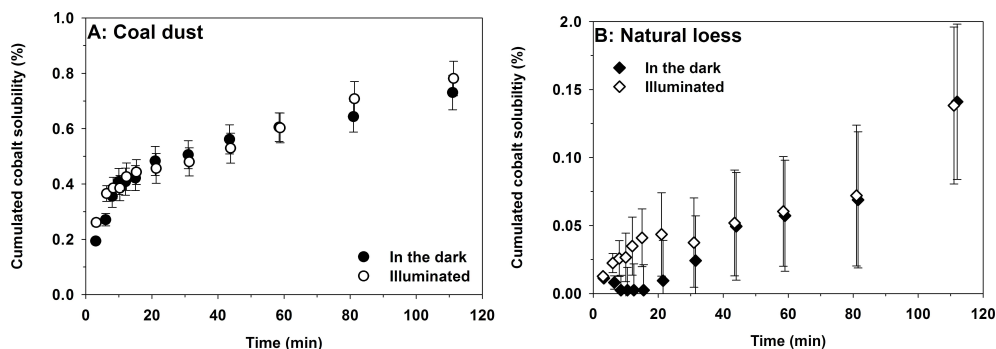

Fig. 3. Cumulated solubility of cobalt (%) as a function of time of the experiment, for anthropogenic (**A**) and natural dusts (**B**).

Table 3. Percentage of dissolved metal from initial composition of the dust (cf. Table 2) after 2 h of dissolution in seawater.

	Light irradiation	Co (%)	Zn (%)
Coal ash dust	No	0.73	N.D.
Coal ash dust	Yes	0.78	5.16
Loess	No	0.14	N.D.
Loess	Yes	0.14	16.27

anthropogenic Co (0.78% after 2 h, Table 3, Annexe 3) than for the natural one (0.14% after 2 h). For anthropogenic Co, no differences between irradiated and dark were seen. But for the natural Co, irradiations seemed to speed up the dissolution rate during the first 30 min. The dissolution processes did not stop after the 2 h of experiment and may continue for longer time. For the loess the difference between irradiated and dark Co was not significant in the dissolution rate graphs (Fig. 2); but the cumulative solubility curve (Fig. 3) showed significant differences at the beginning of the experiment. This was due to a statistical effect because the dissolution rate of Co with irradiation was systematically higher at the beginning of the dissolution experiment.

Plotting the cumulative dissolution rate as function of the square root of the time can highlight similar processes encountered in continuous weathering experiments driven by
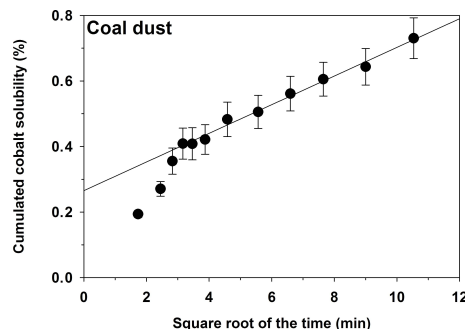

Fig. 4. Cumulated solubility of cobalt (%) as function of square root of the time ($y = 0.044x + 0.265$, $R^2 = 0.991$).

diffusion processes (Wollast, 1967). For anthropogenic Co (Fig. 4), the second part of the cumulative dissolution followed linearly the square root of the time. Extrapolation to 100% of the square root line of the Co dissolution (Table 4) gave a time of 3659 days (10 years) for a total dissolution of Co from the anthropogenic particles.

3.4 Zinc in seawater

The Zn composition for both dusts was very different (Table 2) with 10 times more Zn in anthropogenic than in natural.

Table 4. Extrapolation of the linear correlation between the dissolution of Co (top) and Zn (bottom) as function of the square root of the time. 100% means total dissolution of the metal in seawater.

% Dissolved Co	Extrapolated time (h)	Extrapolated time (day)
10%	840	35
25%	5400	230
50%	22000	920
75%	49000	2200
100%	88000	3700

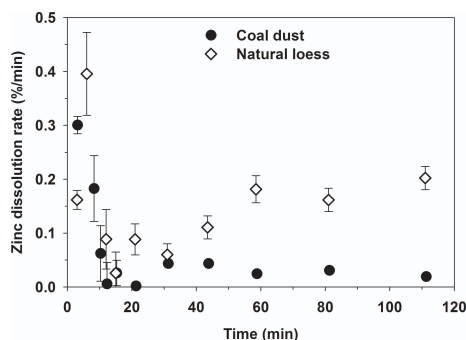| % Dissolved Zn	Extrapolated time (h)	Extrapolated time (day)
10%	6	0.3
25%	36	1.5
50%	140	6
75%	310	13
100%	550	23

Fig. 5. Dissolution rates of zinc (%/min) for anthropogenic and natural dust as function of time.

The dissolution rate shape was also different for both dust types (Fig. 5). The anthropogenic Zn dissolution started with a rate of about 0.3–0.4%/min and then decreased during the first 30 min. Despite a small increase at 30 min for anthropogenic Zn, the dissolution rate remained low (<0.1%/min). But for the natural Zn (Fig. 5), the dissolution rate increased more from 20 min of dissolution and remained at 0.2%/min after 2 h.

The total dissolved Zn from dust after 2 h of experiment (Table 3, Annexe 4) was higher in the natural loess (16.27%) than in the anthropogenic coal ash dust (5.16%) but available quantity was greater for anthropogenic coal ash dust (12 nmol) than natural loess (5 nmol).

Figure 6 represents the cumulative relative dissolution of Zn as function of the time and Fig. 7 as function of the square root of the time. The second part of the second plot (for longer times) showed a linear relationship with the anthropogenic dust, but not with the natural one. The extrapolation of the straight line gave a time of 552 h (23 days) for a total dissolution of Zn from the anthropogenic particles (Table 4).
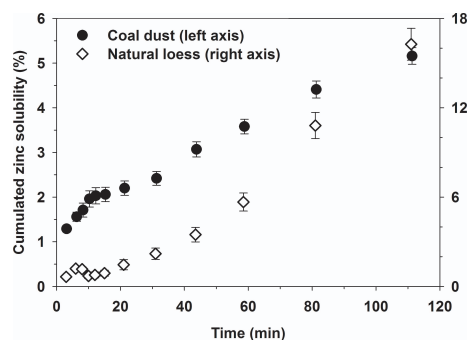

Fig. 6. Cumulated solubility of zinc (%) for anthropogenic and natural dust as a function of time.
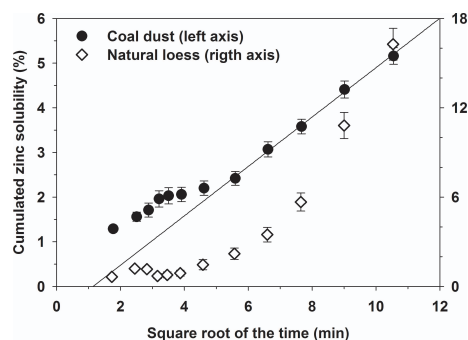

Fig. 7. Cumulated solubility of zinc (%) as function of the square root of time ($y = 0.553x - 0.632$, $R^2 = 0.998$).

4 Discussion

4.1 Solubility features of Co and Zn from dust in seawater

The dissolution experiments in open-flow reactor showed significant differences between the natural soil (loess) and the anthropogenic coal ash dusts: anthropogenic dusts were much more enriched with Zn compared to natural soils (Table 2), but after 2 h of exposure to seawater, the relative amount released was 5.16% compared to 16.27% of natural (Table 3). On the contrary, natural soils had slightly more Co than anthropogenic dusts (Table 2) but they released less of it after 2 h of exposure to seawater (0.14% for the loess against 0.78% for the coal ash dust; Table 3). This is similar to the findings of Sedwick et al. (2007) for iron, with Saharan air containing a relatively high loading of aerosol iron (27.8 nmol Fe/m^3) which had a low fractional solubility (0.44%); reversely, North American air contained a relatively low concentration of aerosol iron (0.5 nmol Fe m^{-3}) which had a high fractional solubility (19%). Differences in the morphology of the dust could account for some of these dissolution features. Indeed based on solubility rates of spherical particles (using the Stokes-Einstein equation), the small spherical particles of coal ash dust should be more

soluble than the particles of the loess (bigger and complexed shapes; Fig. 1), provided the dissolution is proportional to the particles size. This would be the case indeed for Co; but not for Zn (Table 3). Differences in mineralogy could also account for the observed dissolution features. For instance the coal ash dusts were mainly constituted of spheres smaller than 1 μm with a fraction easily exchangeable (75%) and a carbonated structure (<15%) (Guieu et al., 1997; Velay, 2006). The trace metals could thus be weakly bound to this mould. In the coal ash dusts, the refractory Zn phase could represent only <15% of the total structure (Guieu et al., 1997; Velay, 2006). Thus, the Zn contained in coal ash dusts could have quickly dissolved in aqueous solution. In opposite, particles from the natural soils were constituted of quartz, clay, feldspath and pyroxene, in which aluminosilicate mould represents 90% of the whole structure (Ausset, 1996; Ausset et al., 1999; Velay, 2006). In such mineral particles the metals would be strongly bound, preventing from a quick dissolution of the metals such as it has been observed for Co and Zn at the beginning of the dissolution experiments (Figs. 2 and 5). It has been suggested that the dissolution of the loess from Cape Verde takes place within two main steps (Desboeufs et al., 1999; Desboeufs, 2001a). The first one is the dissolution of the most soluble phase by complexation processes: an ion OH^- or H^+ can dissolve the metals from a particle by forming inorganic oxy(hydr)-oxides complexes. Natural organic ligand could also bind the metals released from the particle to form dissolved organic complexes thus stabilizing the metal in the dissolved phase. The second one would be the dissolution of the less soluble phases (silicate phase), which produces a residual layer between the silicate phase and the aqueous solution. At pH of seawater (of about 8–8.2) the hydroxide ions OH^- in seawater would hydrolyze the silicated mould, leading to the second stage of the dissolution reaction. Two dissolution steps of Zn were indeed clearly distinguished for the loess (Fig. 5): a first one just at the beginning of the experiment and a second one starting after 10 min and which appeared to continue beyond 120 min. The increase of Zn and Co solubility after 120 min suggested that the metals were not totally dissolved yet from the loess, and thus that the second step of loess dissolution is most likely a slow process. The square root shape obtained after 1 h of dissolution indicates a continuous and stable weathering process for Co and Zn in the anthropogenic particles. Under natural conditions in seawater, complexation processes by dissolved organic matter could promote some of the dissolution of Co and Zn from dusts as observed here and/or stabilise the metals in the dissolved phase.

4.2 Atmospheric input of cobalt and zinc to surface oceanic waters and its potential biogeochemical impacts

Atmospheric inputs to the surface ocean generally occur during sporadic events. Among them, Saharan events are major source of dust for the North Atlantic Ocean (Guieu et al., 2002a, b). Dusts from Cape Verde can be transported during such events and then deposited on the surface Atlantic Ocean (Jickells et al., 2005). Assuming an atmospheric input to surface waters ranging between 0.002 to 0.1 mg/L of seawater (according to Bonnet and Guieu, 2004) and a mixed layer of 50 m, the Co and Zn atmospheric inputs to surface waters were then calculated by using the dissolution values obtained in this study (Table 5).

Dissolved Co and Zn in seawater from the loess are given as total percentage (Table 3) of metal dissolved after 2 h (relative to the elemental composition, Table 2, Annexe 2). The iron inputs by Saharan dust estimated in Milli-Q enclosed water systems (0.07 to 1 nM Fe; Bonnet and Guieu, 2004) are larger than Co and Zn inputs calculated here for the loess for two strengths of atmospheric event (Table 5). Additionally, Co concentrations in the surface Atlantic layer (0–50 m) would vary between 20 and 30 pM (Saito and Moffett, 2002, 2001) and Zn between 170 and 320 pM (Ellwood and van den Berg, 2000). The Co inputs to the mixed layer calculated here (0.01 to 0.43 pM) are thus small compared to the concentrations found in the North Atlantic, as well as for the Zn inputs (0.51 to 25.48 pM) but the Co and Zn inventory here might already include the dust dissolution effects; thus the dissolution of metals from dusts in surface waters could contribute to the already present Co and Zn inventories (up to 25% and 100%, respectively). This would not be a sufficient Co input to generate a distinct surface maximum. Indeed, sub-surface minima usually observed at 10–20 m depth are due to phytoplankton uptake and remineralisation processes rather than the slow homogenization of the water masses. In the Pacific Ocean, the concentrations of Co and Zn in surface waters (mixed layer) can be below 10 pM for Co and below 50 pM for Zn. Thus, Co input from the natural dust could account for approximately 0.1 to 5% of the concentration naturally present in the mixed layer, and Zn input could account for 1 to 50% of the concentration naturally present in surface waters of the Pacific Ocean.

Atmospheric inputs of dissolved Co to the surface water calculated for a strong dust event (0.43 pM, Table 5) are as high as the inorganic Co (Co') cellular requirement of a calcifying phytoplankton species like *E. huxleyi* (Km~0.6 pM; Sunda and Huntsman, 1995; Xu et al., 2007). Similarly dissolved Zn inputs from the loess (0.51 to 25.48 pM; Table 5) are 5 to 250 times higher than the half-saturation constant of inorganic Zn (Zn') for siliceous species like *T. oceanica* (Km~0.1 pM; Sunda and Huntsman, 1995). Therefore, such atmospheric inputs of Co and Zn have the potential to alleviate growth limitation of *E. huxleyi* and *T. oceanica*, respectively, assuming that the dissolved metal fraction is entirely bio-available. However these estimates were based on dissolution from loess of Cape Verde that may not be the most significant atmospheric source of dusts to the North Atlantic. Complementary studies, especially focusing onto the Saharan events which represent 26% of the total dust input to the

Table 5. Dissolved Co and Zn inputs to a mixed layer (50 m) induced by a weak and a strong atmospheric event and estimated with the percentage of dissolved metal from the dust after 2 h of dissolution in seawater.

Atmospheric event magnitude	Weak	Strong
Final concentration of Saharan dust in a mixed layer* (mg/L)	0.002*	0.1*
Co dissolution from the loess with light (%)	0.14	0.14
Zn dissolution from the loess with light (%)	16.27	16.27
Co input to the mixed layer (pM)	0.01	0.43
Zn input to the mixed layer (pM)	0.51	25.48

* Values of Bonnet and Guieu (2004)

global surface ocean (Jickells et al., 2005) would thus help to further understand the impact of the atmospheric metals inputs on the oceanic phytoplankton, notably in the North Atlantic.

The anthropogenic input to the surface ocean is much more difficult to assess since few or no data is available. However, Sholkovitz et al. (2009) estimated the annual apportionment of soluble iron from anthropogenic aerosol source to be from 70 to 85% of the total aerosol input (natural and anthropogenic) near Bermuda and Ireland. In regions with high natural dust input like near Izana and Barbados, it was about 12% (Sholkovitz et al., 2009). Using the solubility of Co and Zn from the coal ash dust in seawater and its elemental composition obtained in this study (Tables 2 and 3), and using 12% of the total dust concentration in the mixed layer for weak and strong dust event (Table 5), the anthropogenic Co input to the mixed layer (0.01–0.34 pM) would thus be in the same range than the natural Co dust input (0.01–0.43 pM). Reversely, the Zn input to the mixed layer (0.14–7.05 pM) would be 3 times lower than the input from natural dusts (0.51–25.48 pM). However a better estimate of the flux of anthropogenic aerosol to the surface ocean is required to further estimate these anthropogenic inputs. For instance anthropogenic fluxes from the east coast of the United States and from Western Europe to the North Atlantic Ocean would be required.

Variations in natural and anthropogenic inputs between different locations could induce large variations in Co/Zn ratio in surface waters, thus having a potential impact on the phytoplankton community structure. Indeed, diatoms have a higher demand in Zn than Co compared to coccolithophorids that are primarily limited by Co (Sunda and Huntsman, 1995; Saito et al., 2002). Also cyanobacteria, present in abundance in the studied region, strongly prefer Co rather than Zn (Saito et al., 2002). For instance Sunda and Huntsman (1995) showed that the cyanobacteria *Synechococcus bacillaris* has a high cellular requirement for Co, between 0.08 and 1.43 μmol mol^{-1} Co:C. Higher Zn input via natural and/or anthropogenic atmospheric dust would be in favour of diatom communities. Understanding the forcing that drives the distribution of the dominant phytoplank-

ton groups is essential because they have different nutrient utilization characteristics, and they support different marine food webs.

5 Conclusions

This study showed some dissolution processes at the atmosphere-ocean interface of two trace metals poorly studied. Co and Zn play key roles in the functioning of the metabolism of the coccolithophorids, cyanobacteria and diatoms. The originality of this work was the use of an open-flow reactor, which better simulates the phenomenon occurring at the interface atmosphere-ocean, in order to evaluate the solubility of these two trace metals with the time after the dust deposition in surface waters. The experiments described here give an appropriate overview of the quick dissolution of Co and Zn in seawater from the coal ash dust. However, the natural soil showed much slower dissolution of Co and Zn where no extrapolation is possible after the experiment time. Characterization of Co and Zn dissolution from natural and anthropogenic particles in seawater has not been previously reported to our knowledge. This work also helps to determinate the percentage of dissolved metal from the dusts in seawater, and therefore to evaluate the atmospheric inputs to the surface ocean during a dust event. The results showed clear differences between the natural soil and the anthropogenic dusts. The small spherical and carbonated particles of coal ash dust released Zn quickly in seawater, but the quantity was less than the natural soil from Cape Verde with an aluminosilicate mould; whereas opposite trends were observed for Co.

This work can be pursued with the study of other trace metals important for the marine biology like iron, but also with other dusts (such as Saharan dusts) and with longer dissolution experiment in open-flow reactor to better investigate the slow dissolution processes.

Supplementary material related to this article is available online at:
http://www.biogeosciences.net/7/1927/2010/
bg-7-1927-2010-supplement.pdf.

The publication of this article is financed by CNRS-INSU.

References

Ausset, P., Crovisier, J. L., del Monte, M., Furlan, V., Girardet, F., Hammecker, C., Jeannette, D., and Lefevre, R. A.: Experimental study of limestone and sandstone sulphation in polluted realistic conditions: The Lausanne Atmospheric Simulation Chamber (LASC), Atmos. Environ., 30(18), 3197–3207, 1996.

Ausset, P., del Monte, M., and Lefevre, R. A.: Embryonic sulphated black crusts on carbonate rocks in atmospheric simulation chamber and in the field: role of carbonaceous fly-ash, Atmos. Environ., 33(10), 1525–1534, 1999.

Blain, S., Queguiner, B., Armand, L., Belviso, S., Bombled, B., Bopp, L., Bowie, A., Brunet, C., Brussaard, C., Carlotti, F., Christaki, U., Corbiere, A., Durand, I., Ebersbach, F., Fuda, J. L., Garcia, N., Gerringa, L. J. A., Griffiths, B., Guigue, C., Guillerm, C., Jacquet, S., Jeandel, C., Laan, P., Lefevre, D., Lo Monaco, C., Malits, A., Mosseri, J., Obernosterer, I., Park, Y. H., Picheral, M., Pondaven, P., Remenyi, T., Sandroni, V., Sarthou, G., Savoye, N., Scouarnec, L., Souhaut, M., Thuiller, D., Timmermans, K. R., Trull, T., Uitz, J., van Beek, P., Veldhuis, M. J. W., Vincent, D., Viollier, E., Vong, L., and Wagener, T.: Effect of natural iron fertilization on carbon sequestration in the Southern Ocean, Nature, 446(7139), 1070-U1, 2007.

Bonnet, S. and Guieu, C.: Dissolution of atmospheric iron in seawater, Geophys. Res. Lett., 31(3), L03303, doi:10.1029/2003GL018423, 2004.

Chou, L. and Wollast, R.: Study of the weathering of albite at room temperature and pressure with a fluidized bed reactor, Geochim. Cosmochim. Ac., 48(11), 2205–2217, 1984.

Desboeufs, K. V.: Processus de dissolution des aérosols atmosphériques au sein des gouttes d'eau nuageuses, Ph.D. report, Laboratoire Interuniversitaire des Systèmes Atmosphériques (LISA), University Paris 7 Denis Diderot, 224 pp., http://tel.archives-ouvertes.fr/tel-00005175/fr/, 2001.

Desboeufs, K. V., Losno, R., Vimeux, F., and Cholbi, S.: pH dependent dissolution of wind transported Saharan dust, J. Geophys. Res., 104, 21287–21299, 1999.

Desboeufs, K. V., Losno, R., and Colin, J. L.: Factors influencing aerosol solubility during cloud processes, Atmos. Environ., 35(20), 3529–3537, 2001b.

Desboeufs, K. V., Losno, R., and Colin, J. L.: Figures of merit of pneumatic and ultrasonic sample introduction systems in inductively coupled plasma-multichannel-based emission spectrometry in an ultra-clean environment, Anal. Bioanal. Chem., 375(4), 567–573, 2003.

Desboeufs, K. V., Sofikitis, A., Losno, R., Colin, J. L., and Ausset, P.: Dissolution and solubility of trace metals from natural and anthropogenic aerosol particulate matter, Chemosphere, 58(2), 195–203, 2005.

Duce, R. A. and Tindale, N. W.: Atmospheric transport of iron and its deposition in the ocean, Limnol. Oceanogr., 36(8), 1715–1726, 1991.

Ellwood, M. J. and van den Berg, C. M. G.: Zinc speciation in the Northeastern Atlantic Ocean, Mar. Chem., 68(4), 295–306, 2000.

Ellwood, M. J. and van den Berg, C. M. G.: Determination of organic complexation of cobalt in seawater by cathodic stripping voltammetry, Mar. Chem., 75(1–2), 33–47, 2001.

Frausto da Silva, J. J. R. and Williams, R. J. P.: The Biological Chemistry of the Elements, Clarendon Press, Oxford, 561 pp., 1994.

Guieu, C., Chester, R., Nimmo, M., Martin, J.-M., Guerzoni, S., Nicolas, E., Mateu, J., and Keyse, S.: Atmospheric input of dissolved and particulate metals to the Northwestern Mediterranean, Deep-Sea Res. Pt. II, 44(3–4), 655–674, 1997.

Guieu, C., Loye-Pilot, M. D., Ridame, C., and Thomas C.: Chemical characterization of the Saharan dust end-member: Some biogeochemical implications for the Western Mediterranean Sea, J. Geophys. Res.-Atmos., 107(D15), 4258, doi:10.1029/2001JD000582, 2002a.

Guieu, C., Bozec, Y., Blain, S., Ridame, C., Sarthou, G., and Leblond, N.: Impact of high Saharan dust inputs on dissolved iron concentrations in the Mediterranean Sea, Geophys. Res. Lett., 29(19), 1911, doi:10.1029/2001GL014454, 2002b.

Jickells, T. D., An, Z. S., Andersen, K. K., Baker, A. R., Bergametti, G., Brooks, N., Cao, J. J., Boyd, P. W., Duce, R. A., Hunter, K. A., Kawahata, H., Kubilay, N., La Roche, J., Liss, P. S., Mahowald, N., Prospero, J. M., Ridgwell, A. J., Tegen, I., and Torres, R.: Global iron connections between desert dust, ocean biogeochemistry, and climate, Science, 308(5718), 67–71, 2005.

Johnson, K. S., Gordon, R. M., and Coale, K. H.,: What controls dissolved iron concentrations in the world ocean?, Mar. Chem., 57(3–4), 137–161, 1997.

Journet, E., Desboeufs, K. V., Caquineau, S., and Colin, J. L.: Mineralogy as a critical factor of dust iron solubility, Geophys. Res. Lett., 35(7), 47–51, 2008.

Kobayashi, M., Shimizu, S.: Cobalt proteins, Eur. J. Biochem., 261(1), 1–9, 1999.

Noble, A. E., Saito, M. A., Maiti, K., and Benitez-Nelson, C. R.: Cobalt, manganese, and iron near the Hawaiian Islands: A potential concentrating mechanism for cobalt within a cyclonic eddy and implications for the hybrid-type trace metals, Deep-Sea Res. Pt. II, 55(10–13), 1473–1490, 2008.

Saito, M. A. and Moffett, J. W.: Complexation of cobalt by natural organic ligands in the Sargasso Sea as determined by a new high-sensitivity electrochemical cobalt speciation method suitable for open ocean work, Mar. Chem., 75(1–2), 49–68, 2001.

Saito, M. A. and Moffett, J. W.: Temporal and spatial variability of cobalt in the Atlantic Ocean, Geochim. Cosmochim. Ac., 66(11),

1943–1953, 2002.

Saito, M. A., Moffett, J. W., Chisholm, S. W., and Waterbury, J. B.: Cobalt limitation and uptake in *Prochlorococcus*, Limnol. Oceanogr., 47(6), 1629–1636, 2002.

Schulz, K. G., Zondervan, I., Gerringa, L. J. A., Timmermans, K. R., Veldhuis, M. J. W., and Riebesell, U.: Effect of trace metal availability on coccolithophorid calcification, Nature, 430(7000), 673–676, 2004.

Sholkovitz, E. R., Sedwick, P. N., and Church, T. M.: Influence of anthropogenic combustion emissions on the deposition of soluble aerosol iron to the ocean: Empirical estimates for island sites in the North Atlantic, Geochim. Cosmochim. Ac., 73(14), 3981–4003, 2009.

Sunda, W. G. and Huntsman, S. A.: Cobalt and zinc interreplacement in marine phytoplankton: biological and geochemical implications, Limnol. Oceanogr., 40(8), 1404–1417, 1995.

Vallee, B. L. and Auld, D. S.: Zinc coordination, function, and structure of zinc enzymes and other proteins, Biochemistry, 29(24), 5647–5659, 1990.

Velay, J. M.: Ph.D. report, Laboratoire Interuniversitaire des Systèmes Atmosphériques (LISA), University Paris 7 Denis Diderot, 259 pp., 2006.

Westenbrink, W. W., Page, A., Vanloon, G. W.: The voltammetric determination of cobalt(II) in seawater – adsorptive preconcentration of the dimethylglyoxime complex, Can. J. Chem., 68, 209–213, 1990.

Wollast, R.: Kinetics of alteration of K-feldspar in buffered solutions at low temperature, Geochim. Cosmochim. Ac., 31(4), 635–648, 1967.

Xu, Y., Tang, D., Shaked, Y., and Morel, F. M. M.: Zinc, cadmium, and cobalt interreplacement and relative use efficiencies in the coccolithophore *Emiliania huxleyi*, Limnol. Oceanogr., 52(5), 2294–2305, 2007.